

# AE feature analysis on welding crack defects of HG70 steel used by truck crane

Yantao Dou<sup>1</sup>, Xiaoli Xu<sup>2</sup>, Wei Wang<sup>3,\*</sup>, Siqin Pang<sup>1</sup>

<sup>1</sup> Beijing Institute of Technology, Beijing, P. R. China,

<sup>2</sup> Beijing Information Science and Technology University, Beijing, P. R. China,

<sup>3</sup> College of Engineering, China Agricultural University, Beijing, P. R. China

[wxw@me.buaa.edu.cn](mailto:wxw@me.buaa.edu.cn)

**Abstract.** In present paper, using Acoustic Emission (AE) as a ultrasonic technique, Welding crack has been investigated on the HG70 steel used by truck crane during three-point bending test was carried out. The study shows that the activity of AE increases greatly during the welding crack initiates and propagates, and the distributing range of AE characteristic parameters can be fixed. AE signals of welding crack initiation and expansion are typical sudden signals which have a different spectrum energy distribution range with that of unstable crack propagation.

**Key words:** HG70 steel, Welding crack, Acoustic Emission

## 1. Introduction

As an important loading and transporting machine, truck crane is widely used in various fields of national economy. To achieve high efficiency and large scale production, truck cranes are often overloaded, which result in accidents frequently. The main cause lies in the damage of structural parts, for example, boom fracture brought about by fatigue crack or weld defects.

The current popular detecting technologies include macroscopic artificial inspection, ultrasonic testing, magnetic particle testing, radiographic testing, penetrant testing, stress-strain testing and so on, which often fail to have a complete and real-time detection of crane metal structures since they are often used as periodic testing or testing afterwards[4]. Acoustic Emission (AE) technology can just make up the deficiency of conventional detection methods. During the past 20 years, some research works have been carried out to the aerial personnel devices or crane structure[1-3].

The aim of this paper is to investigate the AE signals during three-point bending test of welding specimens made of HG70 steel. The typical characteristic parameters and waveform features of the AE signals are collected and extracted at the three development stages of welding crack, namely as crack initiation, growth and fracture[5], and the crack position was located by way of linear location.

## 2. Preparation

### 2.1. Specimen Preparation

HG70 steel, commonly used in crane booms and legs, is chosen as the experimental material. Table 1 and Table 2 indicate its chemical composition and mechanics properties[6].

**Table 1** Chemical composition of HG70

Chemical Composition (weight fraction %)								
C	Si	Mn	P	S	Mo	Cr	Nb	V
0.06	0.29	1.56	0.014	0.008	0.33	0.61	0.04	0.04

**Table 2** Mechanics properties of HG70

$\sigma_s / MPa$	$\sigma_b / MPa$	$\sigma_5 (\%)$	$A_{KV} / J$
570	725	26	69

The structure of welding specimens is shown in Fig 1. The welding interface is located in the middle of the specimens. The specimens are loaded through three-point bending mode.

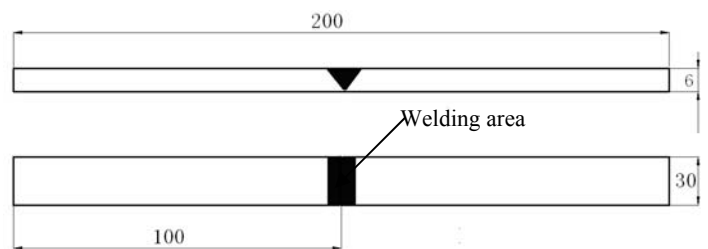


**Fig.1.**Structure of welding specimens

### 2.2. Test equipment and the placement of sensors

Computer controlled electro-hydraulic servo universal test machine of WDW4200 Series is adopted for the loading test, with its max. test force being 200kN, and the indicating accuracy:  $\pm 0.5\%$ . Besides, AMSY-5 AE-System by Vallen and VSI50-M sensors are chosen for the test. The sensor's main monitoring

frequency ranges from 100 to 450kHz, and the acquired AE signals are amplified by a 34 dB fixed gain preamplifier (AEP4). The background noise under operation is found to be always below 35dB, which indicates that we can choose the voltage threshold as 40dB. With the test objects being small metal specimens, system timing parameters are specified as PDT: 300 $\mu$ s, HDT: 600 $\mu$ s and HLT: 1000 $\mu$ s. As shown in Fig 2, sensor 1 and sensor 2, placed on the same side of the specimens, provide linear location, which can obtain the AE characteristic parameters, waveform datas and AE locating features of the crack source during the loading time.

### 2.3. Loading course and process

The loading test is shown in Fig 3. To eliminate the noise caused by the friction between the specimen and the support roller, a rubber pad is placed between them. At the beginning of the loading, the specimen is preloaded and unloaded three times to achieve a close contact between the specimen, rubber pad and the support roller. During the whole course, the specimens are always at the stage of elastic deformation. The speed of loading and unloading of the test machine is 1mm/min. The final testing aim is to bend the specimens at  $\alpha \leq 130^\circ$  when a macro crack can be seen by the eye. The AE signals during the whole course are collected and analyzed.

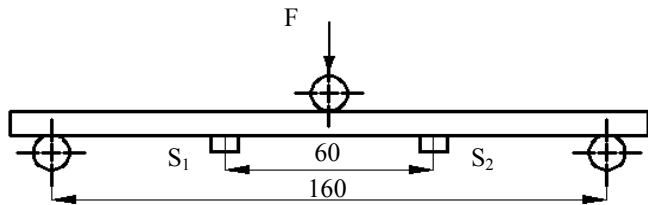


Fig.2. Placement of sensors

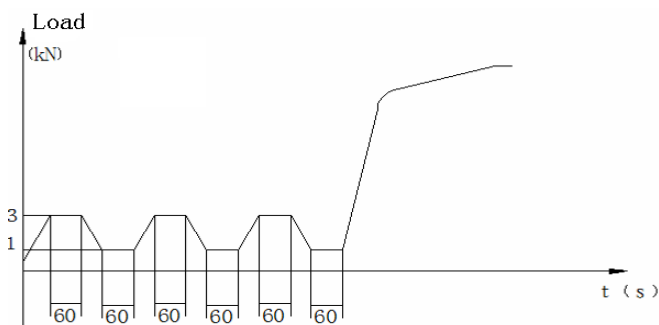
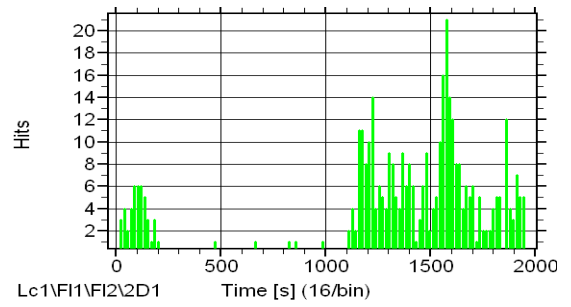


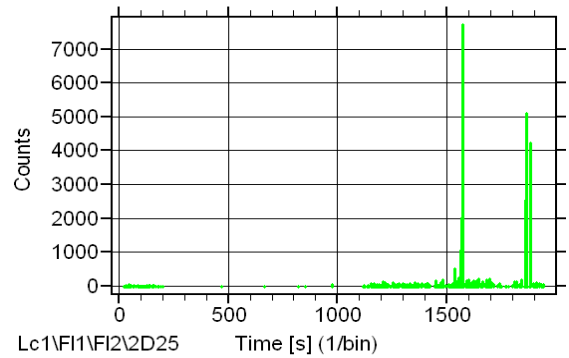
Fig.3. The loading test

## 3. Analysis of AE signals

### 3.1. Analysis of hits and counts versus time



(a) Hits versus time

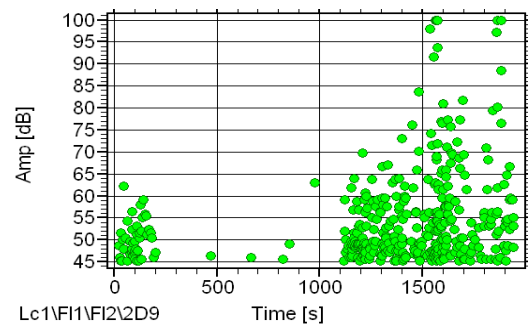


(b) Counts versus time

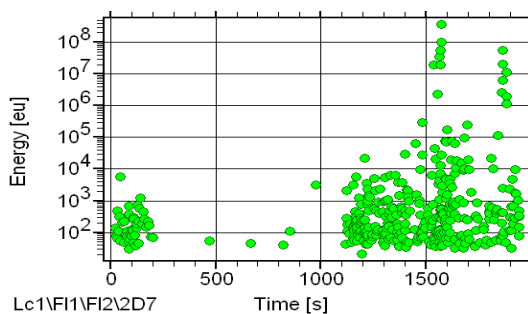
Fig.4. Hits and counts versus time

As shown in Fig 4, a few AE hits are collected at the first preloading stage with rather low counts rates. When first preloaded (0~200s), the specimen undergoes elastic deformation (disturbance below 1mm) with little release of strain energy and the deformation within the material will vanish after unloading, so only a few AE signals are created which include those created by the deformation of the rubber pad and the friction as well as the agreement between the specimen and the support roller. At the 2<sup>nd</sup> and 3<sup>rd</sup> stage of loading, holding load and unloading (400~1100s), no obvious AE signals can be seen. This is partly due to Kaiser Effect, but on the other hand, it signifies there is an agreement between the specimen, rubber pad and support roller where no friction noise is produced. At the last loading (after 1100s), AE hits rates and counts rates increase rapidly, which is caused by the stress concentration in the defect area resulting from the increase of load. In part of the specimens, yield deformation occurs and tiny crack appears and propagates. With the gradual release of internal energy, a large number of AE signals are created.

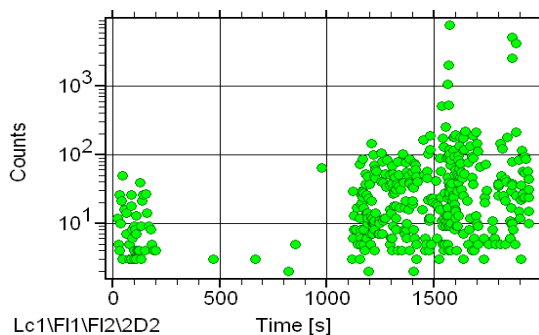
### 3.2. Analysis of AE characteristic parameters versus time



(a) Amplitude versus time



(b) Energy versus time



(c) Counts versus time

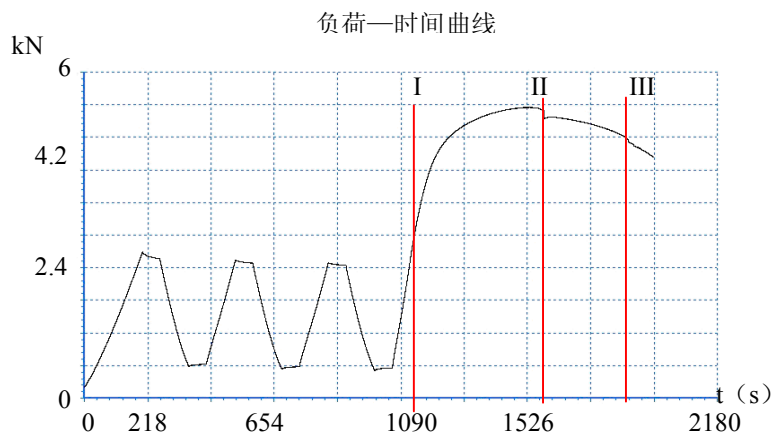
**Fig.5.** AE characteristic parameters versus time

Fig 5 shows the variation of AE characteristic parameters in the loading. At the elastic deformation stage, the value of AE characteristic parameters is rather low, with the amplitude below 60dB, energy below  $10^3$ eu and the counts below 100. When the loading comes to the stage of plastic deformation and crack initiation and propagation, AE hits gradually increase with fairly high amplitude, energy and counts. A number of high-amplitude and high-energy hits even occur simultaneously in some short-time periods, which is caused by the propagation of welding crack.

## 4. Analysis of AE signal features at the welding crack initiation and propagation stage

### 4.1. Analysis of cumulative hits and counts

Fig 6 exhibits its loading-time curve during the test, whereas Fig 7 & 8 respectively show the cumulative hits and counts of AE signals. A comparative study of the three Figs shows the findings: the curve indicates that the specimen enters the stage of part plastic deformation at around 1130s(I). A tiny crack occurs in the welding area and grows gradually due to the stress concentration, which dwindles the load-carrying cross section. When the loading comes to 1570s (II), the crack expands with a snap and the carry capacity falls instantly. The welding crack expands again at 1865s (III). Fig 7&8 show the two instant increases in the value which coincide with the time of the instant fracture of the metal. The findings prove that AE technology can accurately monitor the expansion of welding crack.



**Fig.6.** Loading-time Curve

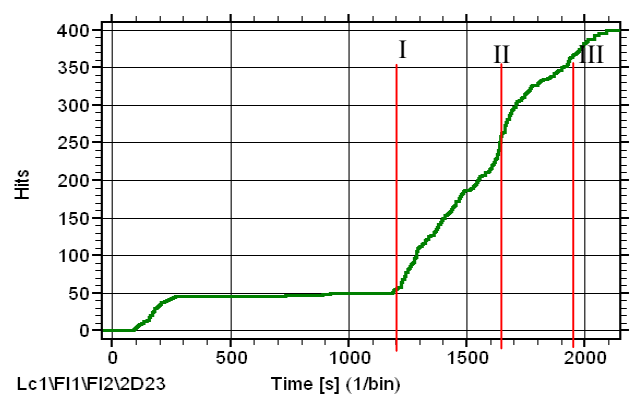


**Fig.7.** Cumulative hits versus time

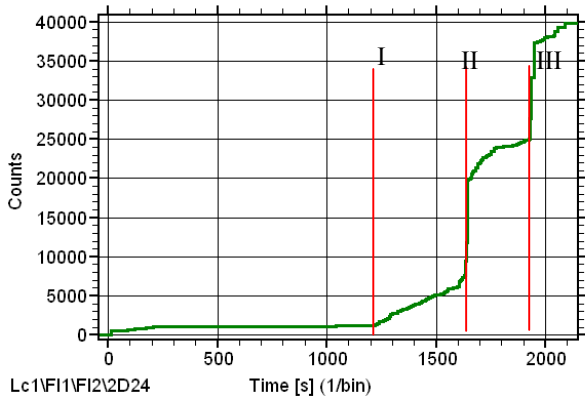


Fig.8. Cumulative counts versus time

#### 4.2. Analysis of AE signal location

Since the initiation and propagation of welding crack is accompanied by rather active AE signals with high amplitude, the amplitude can be amplified to 45dB to filter waves and observe location events. As shown in Fig 9, location events take place mostly in the range of 25~35mm. AE signal location deviation being considered, this range accords with the welding crack location by and large, which sufficiently testify to the location accuracy of AE technology in monitoring welding crack. Fig 10 indicates that location events mainly take place at the time of crack initiation and propagation, which further proves the close relation between middle location events and welding crack.

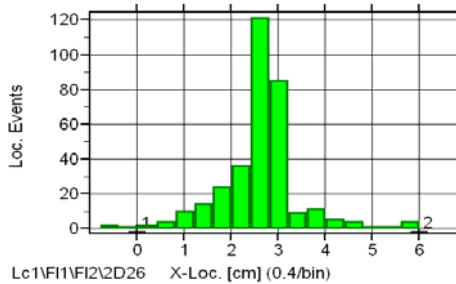


Fig.9. AE location

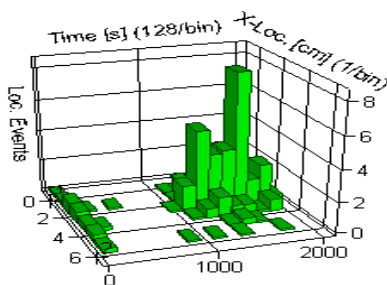


Fig.10. Loc. Events—Time—X-Loc.

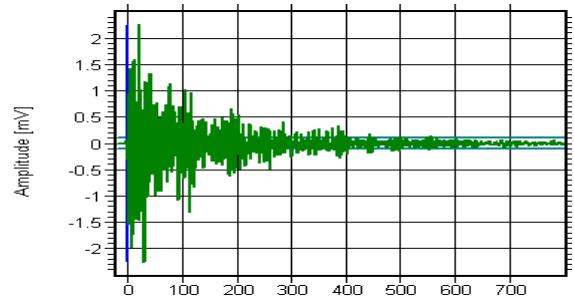
Space filtering ( $25mm \leq x \leq 35mm$ ) and time filtering ( $t \geq 1130s$ ) are adopted to extract the typical AE signals of welding crack initiation and expansion. The distribution and range of characteristic parameters are respectively shown in Table 3.

Table 3. Range of the AE characteristics of welding crack

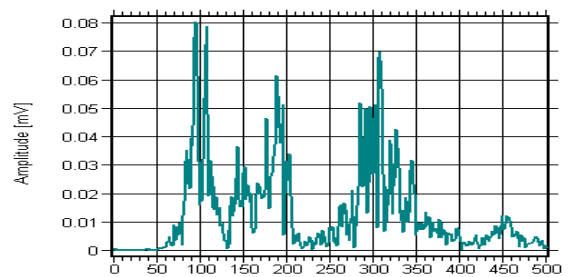
Characteristics	Amplitude (dB)	Counts	Energy (eu)	Duration-Time ( $\mu s$ )
Range	45~100	1~2800	35~ $10^8$	10~2040
Major Range	45~70, 97~100	1~200	40~ 80000	100~1200

#### 4.3. Analysis of time domain waveform and frequency spectrum features at the stage of tip crack and crack propagation

The welding crack develops through three stages: initiation of tiny crack, crack stable propagation and rapid fracture[5]. Fig 11 exhibit the waveform of AE signals at the first and second stage. The time domain waveform Fig shows that the AE signals are typical sudden ones. The frequency spectrum energy of the signals ranges from 80kHz to 380kHz with three major frequency bands: the 1<sup>st</sup> band centers on 100kHz, the 2<sup>nd</sup> from 150kHz to 200kHz and the 3<sup>rd</sup> on 300kHz. The 1<sup>st</sup> and 3<sup>rd</sup> band see rather high energy and obvious peak value.



(a) Waveform



(b) Frequency spectrum

**Fig.11.** Waveform and frequency spectrum of initiation of tiny crack

At the moment of rapid fracture, a few signals of full amplitude (almost 100dB) and high energy ( $10^7 \sim 10^8$ eu) are created as shown in Fig 12. The time domain waveform shows that they are continuous signals formed by several sudden signals which are created by several crack sources. These crack sources are caused by the rapid propagation of the welding crack. As shown in the frequency spectrum Fig 12(b), the frequencies are of rich components and well-distributed between 85kHz and 330kHz. The peak frequencies occur at 100kHz and 200kHz. No obvious peak is shown in high frequency band.

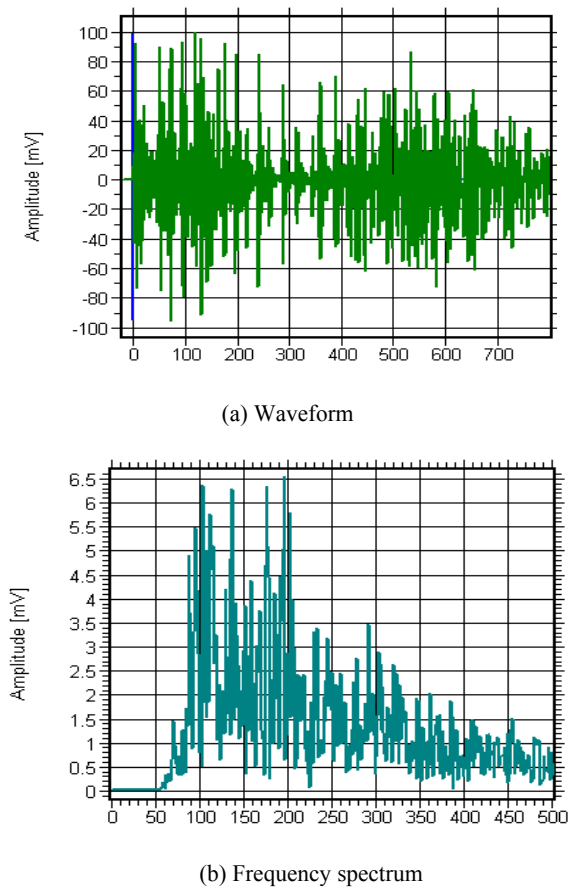


**Fig.12.** Waveform and frequency spectrum of rapid fracture

## 5. Conclusion

Acoustic emission during three-bending tests of welding specimens of HG70 steel were investigated and it was found that AE hits and counts can coincide with the bending and cracking of the specimens. Based on AE hits and counts as well as the loading-time curve of the specimens, welding crack can be dynamically monitored and evaluated.

By way of linear location, the welding crack in the specimens can be accurately located, and the distribution ranges of various AE characteristic parameters at the stage of crack initiation and propagation are tentatively fixed.

The AE signals at the stage of crack initiation and propagation are typical sudden signals whose frequency spectrum energy distributes between 80kHz and 380kHz. Obvious peak value is found at 100kHz and 300kHz. The AE signals at the stage of crack rapid propagation are continuous signals formed by several sudden signals with rich frequency components, but no obvious peak is shown in high frequency band.

## Acknowledgments

This study was funded by National High Technology Research and Development Program of China (2008AA042801, 2008AA042803).

## References:

- [1] WU ZhanWen, SHEN GongTian, WANG ShaoMei.: Characteristics of Acoustic Emission Testing During the Propagating of External Crack on the Crane Box Beam. *Nondestructive Testing*. 30(9), 635-639 (2008)
- [2] ASTM F9 14-03, Standard Test Method for Acoustic Emission for Insulated and Non-Insulated Aerial Personnel Devices Without Supplemental Load Handling Attachments. 9(10), (2003)
- [3] Gordon, R., Drummond, Kevin., F., Fraser., John., Little., et al.: Assessing the structure integrity of crane booms using acoustic emission[C]. EWGAE: 25th European Conference on Acoustic Emission Testing Prague. Czech Republic. (2002)
- [4] WU ZhanWen, SHEN GongTian, WANG ShaoMei.: Application status of acoustic emission technology to crane's nondestructive test. *Hoisting and conveying machinery*. 10, 1-4 (2007)
- [5] C.Ennaceur, A.Laksimi, C.Herve, M.Cherfaoui Monitoring crack growth in pressure vessel steels by the acoustic emission technique and the method of potential difference, *International Journal of Pressure Vessels and Piping*. 83, 197~204 (2006)
- [6] Sheng GuangMin, Gao ChangYin.: Weldability of HG70 steel *Transactions of the china welding institution*. 25(3), 117~119 (2004)
- [7] Meysam Akbari, Mehdi Ahmadi. The application of acoustic emission technique to plastic deformation of low carbon steel *International Congress on Ultrasonics*, Universidad de Santiago de Chile. (1):795~801 (2009)
- [8] XU ChangHang, LIU LiQun, CHEN GuoMing.: Characteristics analysis of acoustic emission signals from steel specimens under tensile fracture and fatigue crack condition. *Journal of China University of Petroleum*. 33(5), 95-99 (2009)
- [9] S H Carpenter, M R Gorman.: A Waveform Investigation of Acoustic Emission Generated during the Deformation and

Cracking of 7075 Aluminum . In : Progress in Acoustic Emission VII, The Japanese Society for NDI. Japan, 105-112 (1994)

[10] QIN Guo-dong, LIU Zhi-ming, WANG Wen-jing.: Study on Acoustic Emission Characteristics of 16Mn Steel in Fatigue Test. China Safety Science Journal. 15(8),105-109. (2005)

[11] ZHOU Jie, MAO Han-ling, HUANG Zhen-feng.: Acoustic emission technique for the detecting of metal fatigue fracture [J]. China Measurement Technology. 33(3), 7-9 (2007) [12] T.M.Roberts ,M.Talebzadeh Fatigue life prediction based on crack propagation and acoustic emission count rates, Journal of Constructional Steel Research. 59(9), 681-693 (2003)